

Simplified Limits on Resonances at the LHC

Elizabeth H. Simmons
Michigan State University
May 8, 2017

with R.S. Chivukula, P. Ittisamai, and K.A. Mohan

Phys. Rev. 94 (2016) 094029
and work in preparation



May 8-10, 2017
University of Pittsburgh

Pheno 2017
Building on the new data

Pheno 2017 is supported by the US DOE, NSF, and PITT PACC

Latest topics in particle physics and related issues in astrophysics and cosmology

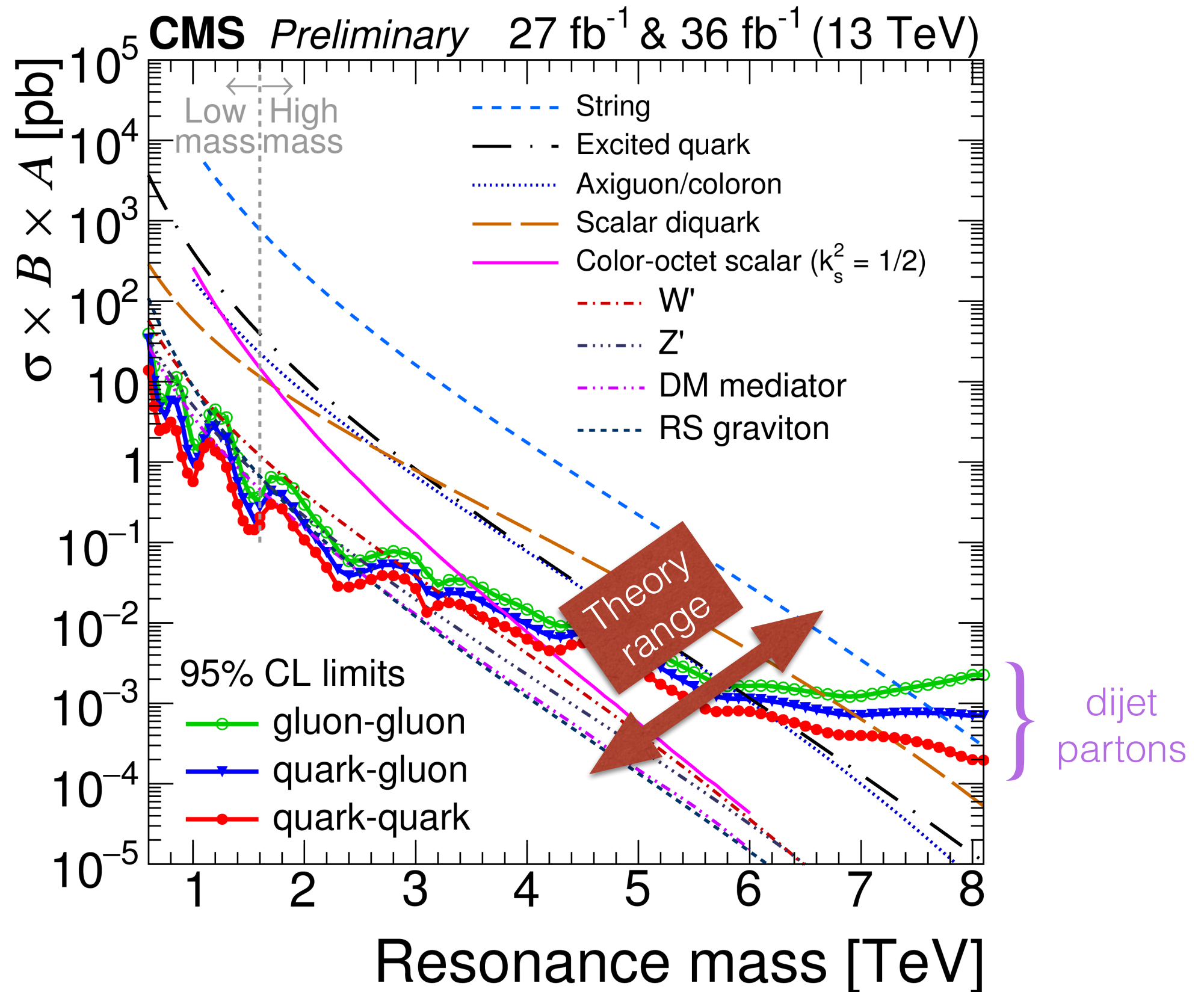
Organizers: Brian Ballew, Cindy Carlson, Ayres Freitas, Dorival Goncalves, Tao Han (chair), Ahmed Ismail, Adam Leibovich, David McKeen, Satyanarayan Mukhopadhyay, Brock Tweedle

Program Advisors: Vernon Barger, Lisa Everett, Koko Higashimura, Arthur Kosowsky, Yao-Yuan Mao, Timon Pahn, Xuesi Tan, Andrew Zentner, Dieter Zeppenfeld

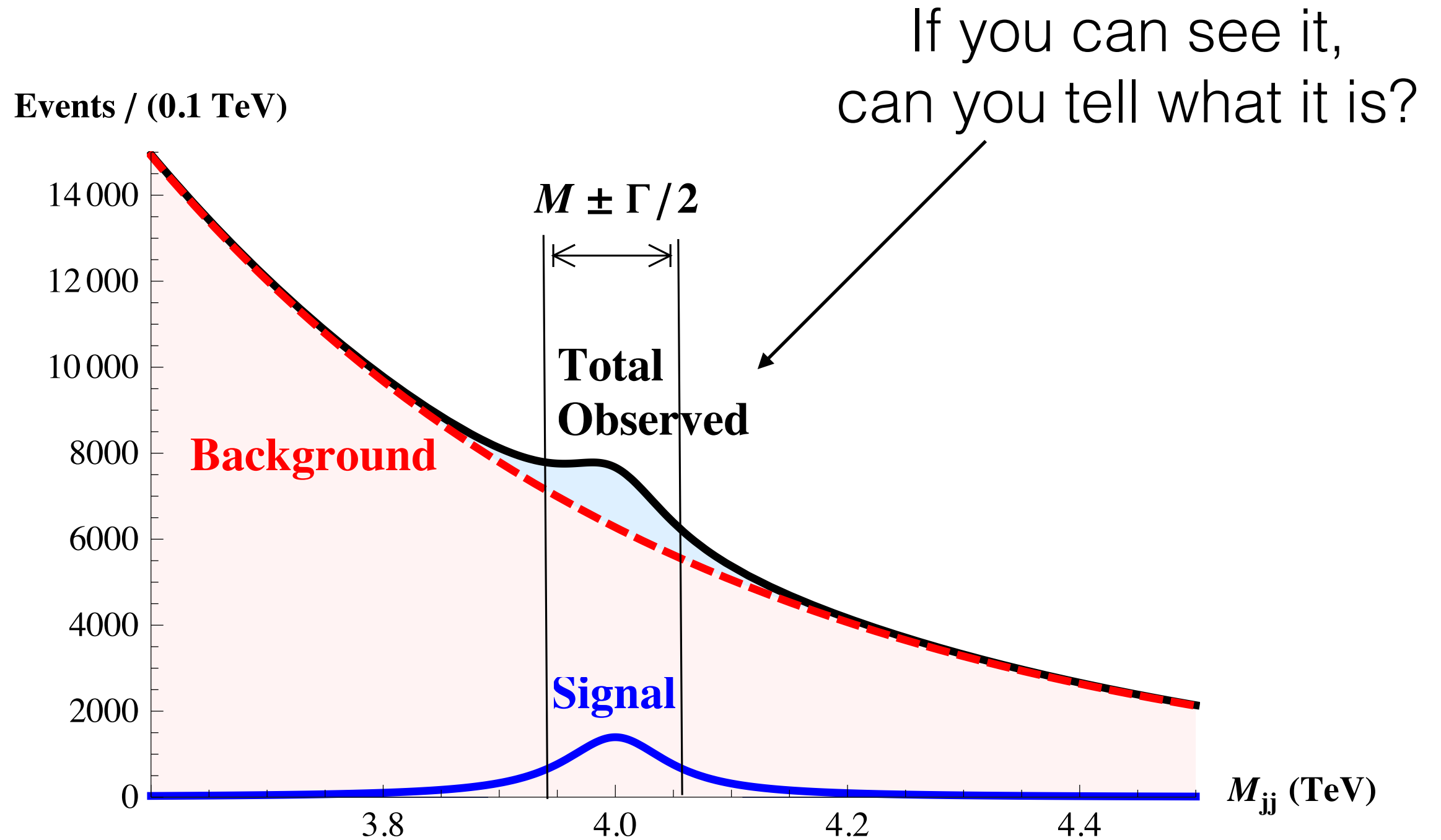
indico.oern.ch/e/pheno17

The Usual Suspects: Dijet Resonances

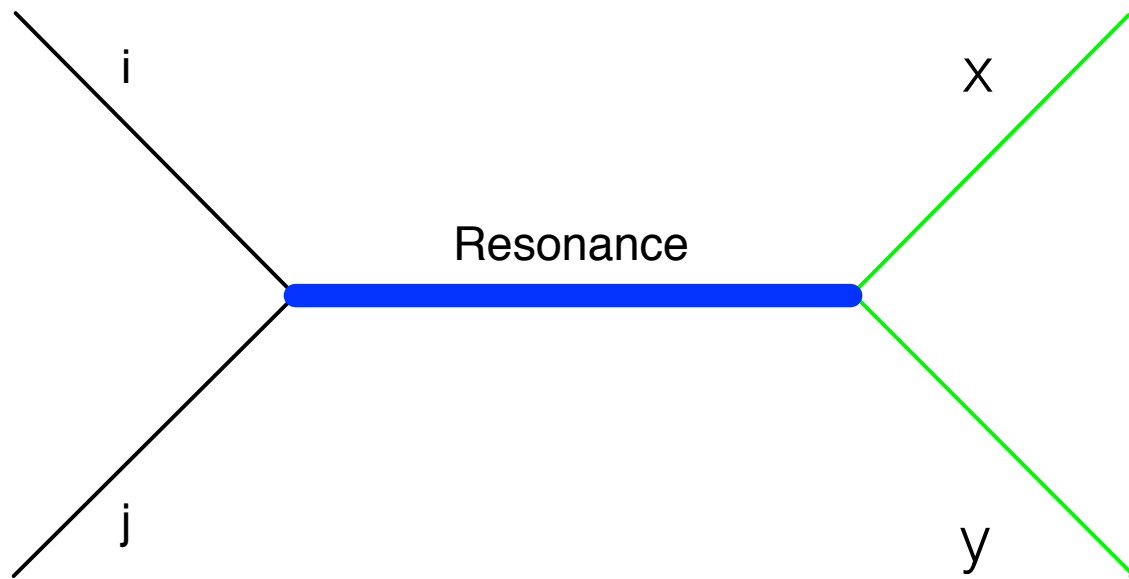
How to represent a broader class of models?



s-channel Resonance



Simplified s-channel Model



$\mathbf{i, j} = u, d, g, \gamma, W, Z$

$\mathbf{x, y} = j, t, b, g, \gamma, W, Z, h$

Resonance Characteristics	Corresponding Observables
couplings	BR, $\sigma^* \text{ BR}$
mass, width	$d\sigma/dm_{ab}$
spin	$d\sigma/d\cos\theta_{ab}$
x, y (each channel)	flavor tagging; jet substructure
i, j	event properties

NB: If x, y can be light quarks,
t-channel process may be relevant

Narrow Width Approximation

$$\sigma_R(pp \rightarrow x + y) = \int_{s_{min}}^{s_{max}} d\hat{s} \hat{\sigma}(\hat{s}) \cdot \left[\frac{dL^{ij}}{d\hat{s}} \right]$$

$$\hat{\sigma}_{ij \rightarrow R \rightarrow xy}(\hat{s}) = 16\pi(1 + \delta_{ij}) \cdot \mathcal{N} \cdot \frac{\Gamma(R \rightarrow i + j) \cdot \Gamma(R \rightarrow x + y)}{(\hat{s} - m_R^2)^2 + m_R^2 \Gamma_R^2}, \quad \mathcal{N} = \frac{N_{S_R}}{N_{S_i} N_{S_j}} \cdot \frac{C_R}{C_i C_j}$$

$$\frac{1}{(\hat{s} - m_R^2)^2 + m_R^2 \Gamma_R^2} \approx \frac{\pi}{m_R \Gamma_R} \delta(\hat{s} - m_R^2)$$

$$\sigma_R(pp \rightarrow x + y) = 16\pi^2 \cdot \mathcal{N} \cdot \frac{\Gamma_R}{m_R} \cdot (1 + \delta_{ij}) BR(R \rightarrow ij) \cdot BR(R \rightarrow xy) \left[\frac{1}{s} \frac{dL^{ij}}{d\tau} \right]_{\tau = \frac{m_R^2}{s}}$$

(Note: Can be corrected for K-factor(s) & Acceptance)

Branching Ratios

$$\sigma_R(pp \rightarrow x + y) = 16\pi^2 \cdot \mathcal{N} \cdot \frac{\Gamma_R}{m_R} \cdot (1 + \delta_{ij}) BR(R \rightarrow ij) \cdot BR(R \rightarrow xy) \left[\frac{1}{s} \frac{dL^{ij}}{d\tau} \right]_{\tau = \frac{m_R^2}{s}}$$

Simplest case: one relevant incoming / outgoing state

$$BR(R \rightarrow i + j)(1 + \delta_{ij}) \cdot BR(R \rightarrow x + y) = \frac{\sigma_R^{xy}}{16\pi^2 \mathcal{N} \frac{\Gamma_R}{m_R} \left[\frac{1}{s} \frac{dL^{ij}}{d\tau} \right]_{\tau = \frac{m_R^2}{s}}}$$

$$\leq 1/4 \quad (ij \rightarrow R \rightarrow xy)$$

$$\leq 1 \quad (ij \rightarrow R \rightarrow ij)$$

$$\leq 1/2 \quad (ii \rightarrow R \rightarrow xy)$$

$$\leq 2 \quad (ii \rightarrow R \rightarrow ii)$$

Upper bound on product of BR shows which classes of models are viable.

Better Variable: ζ

$$\sigma_R(pp \rightarrow x + y) = 16\pi^2 \cdot \mathcal{N} \cdot \frac{\Gamma_R}{m_R} \cdot (1 + \delta_{ij}) BR(R \rightarrow ij) \cdot BR(R \rightarrow xy) \left[\frac{1}{s} \frac{dL^{ij}}{d\tau} \right]_{\tau = \frac{m_R^2}{s}}$$

Simplest case: one relevant incoming / outgoing state

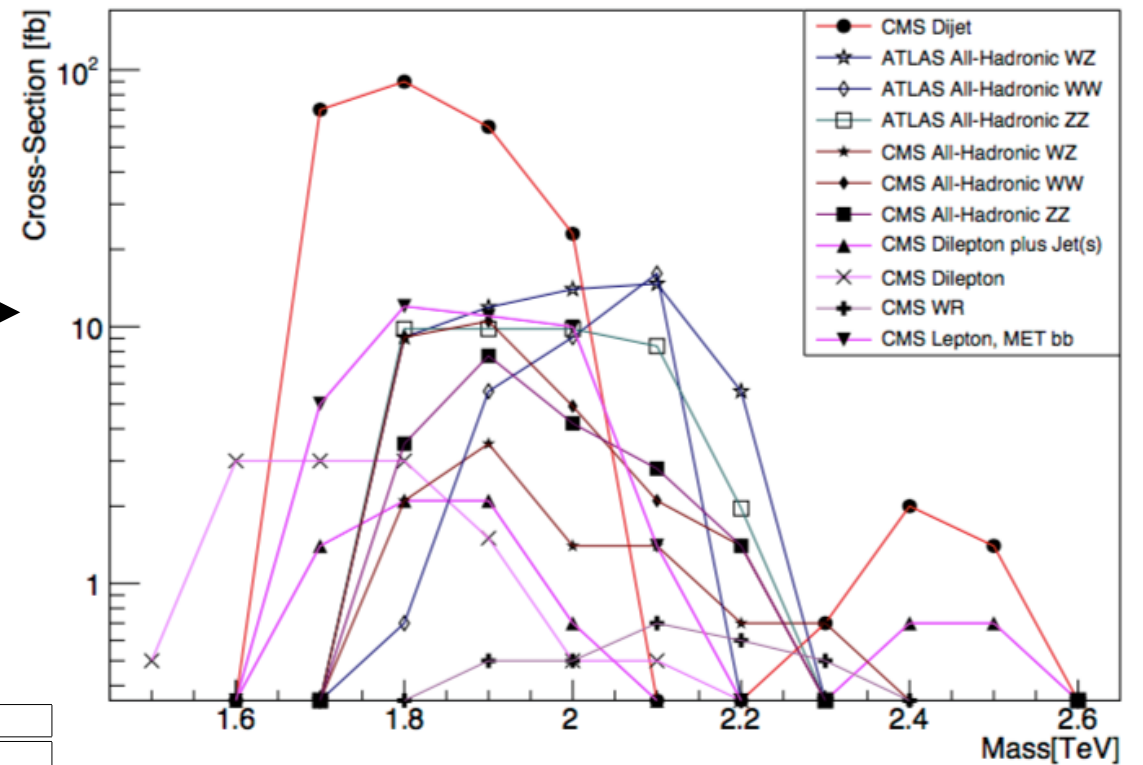
$$\begin{aligned} \zeta &\equiv (1 + \delta_{ij}) BR(R \rightarrow i + j) \cdot BR(R \rightarrow x + y) \cdot \frac{\Gamma_R}{m_R} \\ &= \frac{\sigma_R^{XY}}{16\pi^2 \cdot \mathcal{N} \times \left[\left[\frac{1}{s} \frac{dL^{ij}}{d\tau} \right]_{\tau = \frac{m_R^2}{s}} \right]} \end{aligned}$$

- Collapses different widths onto a single curve
- For upper bound, use $\Gamma/M \sim 0.1$

Memory Lane: DiBoson Excess

1-100 fb
 “WZ” excess ? data? →

↓
 models?



**Les Houches
 Pre-Proceeding 2015**
 The Diboson Excess:
 Experimental Situation and
 Classification of Experiments
arXiv:1512.04537

Spin-1 triplets (V^\pm, V^0)

Prod.	WW	ZZ	WZ	Wh	Zh	γh	$W\gamma$	Z γ	$\gamma\gamma$	gg	hh	$\bar{Q}_3 Q_3$	$\bar{q}q$	ll	$\ell^\pm \nu$	X	Ref.
DY	✓		✓									(✓)	(✓)	(✓)	(✓)		[39, 140–142]
DY	✓		✓	✓	✓							$\sqrt{\bar{q}q}$	✓	(✓)	(✓)		[40, 42, 43, 111]
DY	✓		✓	✓	✓							(✓)	(✓)	(✓)	(✓)		[44]
DY	✓		✓	✓	✓							$\sqrt{\bar{q}q}$	✓	(✓)	(✓)	(✓)	[112]
DY	✓		✓	\sqrt{WZ}	\sqrt{WW}							$\sqrt{\bar{q}q}$	✓	(✓)	(✓)		[45, 46, 85, 91]
DY	✓		✓	\sqrt{WZ}	\sqrt{WW}							✓	✓	(✓)	(✓)		[41]

Spin-1 V^0

Prod.	WW	ZZ	WZ	Wh	Zh	γh	$W\gamma$	Z γ	$\gamma\gamma$	gg	hh	$\bar{Q}_3 Q_3$	$\bar{q}q$	ll	$\ell^\pm \nu$	X	Ref.
DY	✓				\sqrt{WW}							$\sqrt{\bar{q}q}$	✓				[84]
DY	✓				\sqrt{WW}							$\sqrt{\bar{q}q}$	✓	✓			[117]
DY	✓	✓						✓				$\sqrt{\bar{q}q}$	✓				[118]

Spin-1 V^\pm

Prod.	WW	ZZ	WZ	Wh	Zh	γh	$W\gamma$	Z γ	$\gamma\gamma$	gg	hh	$\bar{Q}_3 Q_3$	$\bar{q}q$	ll	$\ell^\pm \nu$	X	Ref.
DY			✓	\sqrt{WZ}								$\sqrt{\bar{q}q}$	✓			✓	[86, 90, 92–94]
DY			✓	\sqrt{WZ}								$\sqrt{\bar{q}q}$	✓				[87, 88]

Scalar

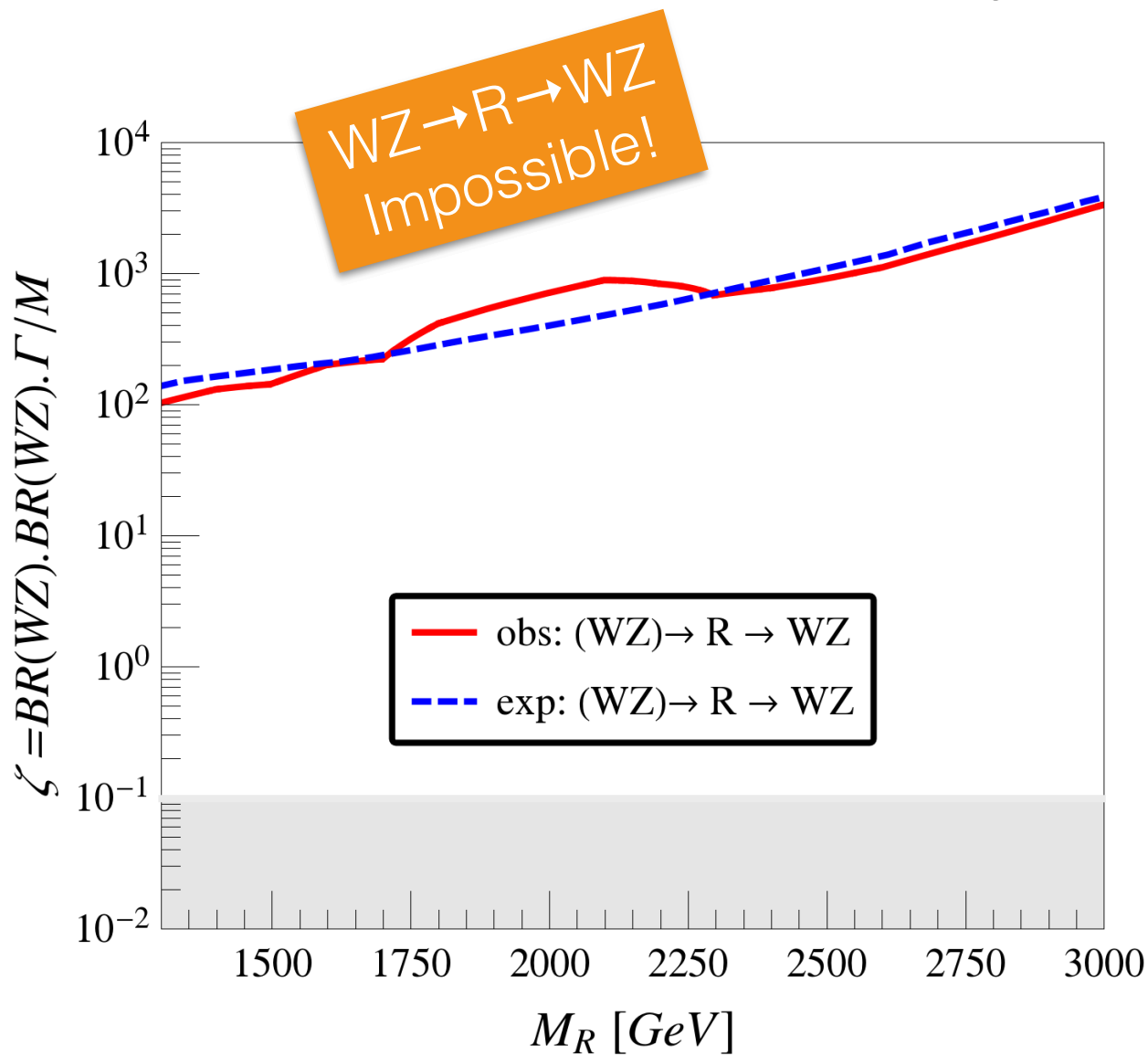
Prod.	WW	ZZ	WZ	Wh	Zh	γh	$W\gamma$	Z γ	$\gamma\gamma$	gg	hh	$\bar{Q}_3 Q_3$	$\bar{q}q$	ll	$\ell^\pm \nu$	X	Ref.
gg	✓	✓						✓	✓	✓							[75, 131, 143]
gg	✓	✓						(✓)	(✓)	✓	$\sqrt{WW/2}$	(✓)					[73]
gg	✓	$\sqrt{WW/2}$				✓			✓	✓	✓	✓				(✓)	[141]
$q\bar{q}$	✓	$\sqrt{WW/2}$		(✓)	(✓)						✓		✓			✓	[123–125]

‘Unconventional’

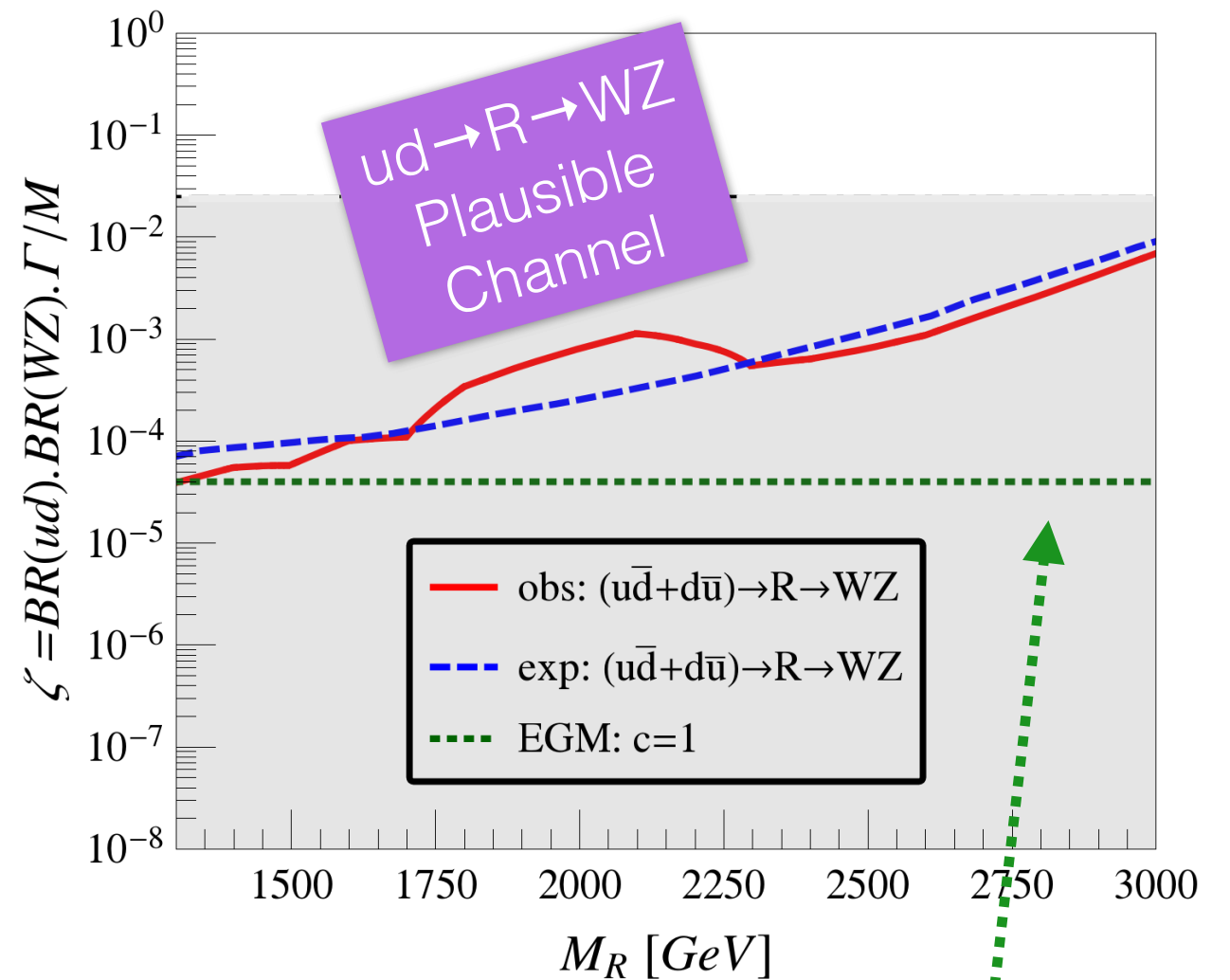
Torsion-free Einstein-Cartan theory																	[144]
Tri-boson interpretation: $pp \rightarrow R \rightarrow VY \rightarrow VV'X$																	[136]
[Implications in other observables (direct and indirect)]																	[95, 97, 142, 145–148]
[Next to leading order predictions]																	[148]
[Analysis techniques]																	[102, 106, 149, 150]

DiBoson Vector Resonances

ATLAS 95% c.l. upper bounds from 20.3 fb⁻¹ at 8 TeV
JHEP **12**, 055 (2015)



In shaded region, ζ has physically allowed value



Extended Gauge Model would not explain excess

Multiple Production and Decay Modes

Easy to evaluate for any model class or model

$$\zeta \equiv \left[\sum_{i'j'} (1 + \delta_{i'j'}) BR(R \rightarrow i' + j') \right] \cdot \left(\sum_{xy \in XY} BR(R \rightarrow x + y) \right) \cdot \frac{\Gamma_R}{m_R}$$

$$= \frac{\sigma_R^{XY}}{16\pi^2 \cdot \mathcal{N} \times \left[\sum_{ij} \omega_{ij} \left[\frac{1}{s} \frac{dL^{ij}}{d\tau} \right]_{\tau = \frac{m_R^2}{s}} \right]}$$

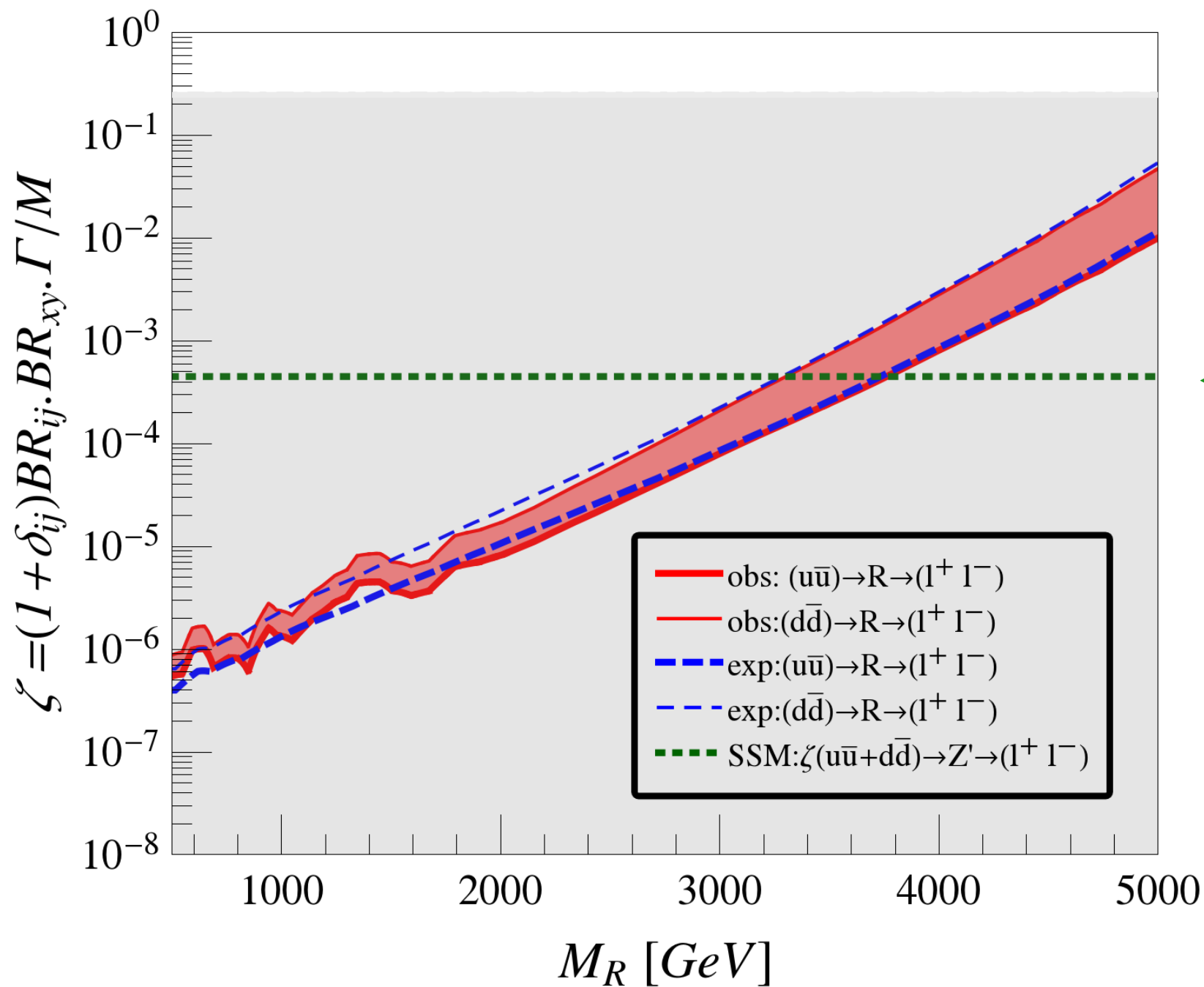
Reporting experimental limits in this format simplifies comparison with theory

weighting factor

$$\omega_{ij} \equiv \frac{(1 + \delta_{ij}) BR(R \rightarrow i + j)}{\sum_{i'j'} (1 + \delta_{i'j'}) BR(R \rightarrow i' + j')}$$

Vector Resonance in Dilepton Channel

ATLAS 95% c.l. upper bounds from 3.2 fb⁻¹ at 13 TeV
ATLAS-CONF-2015-070

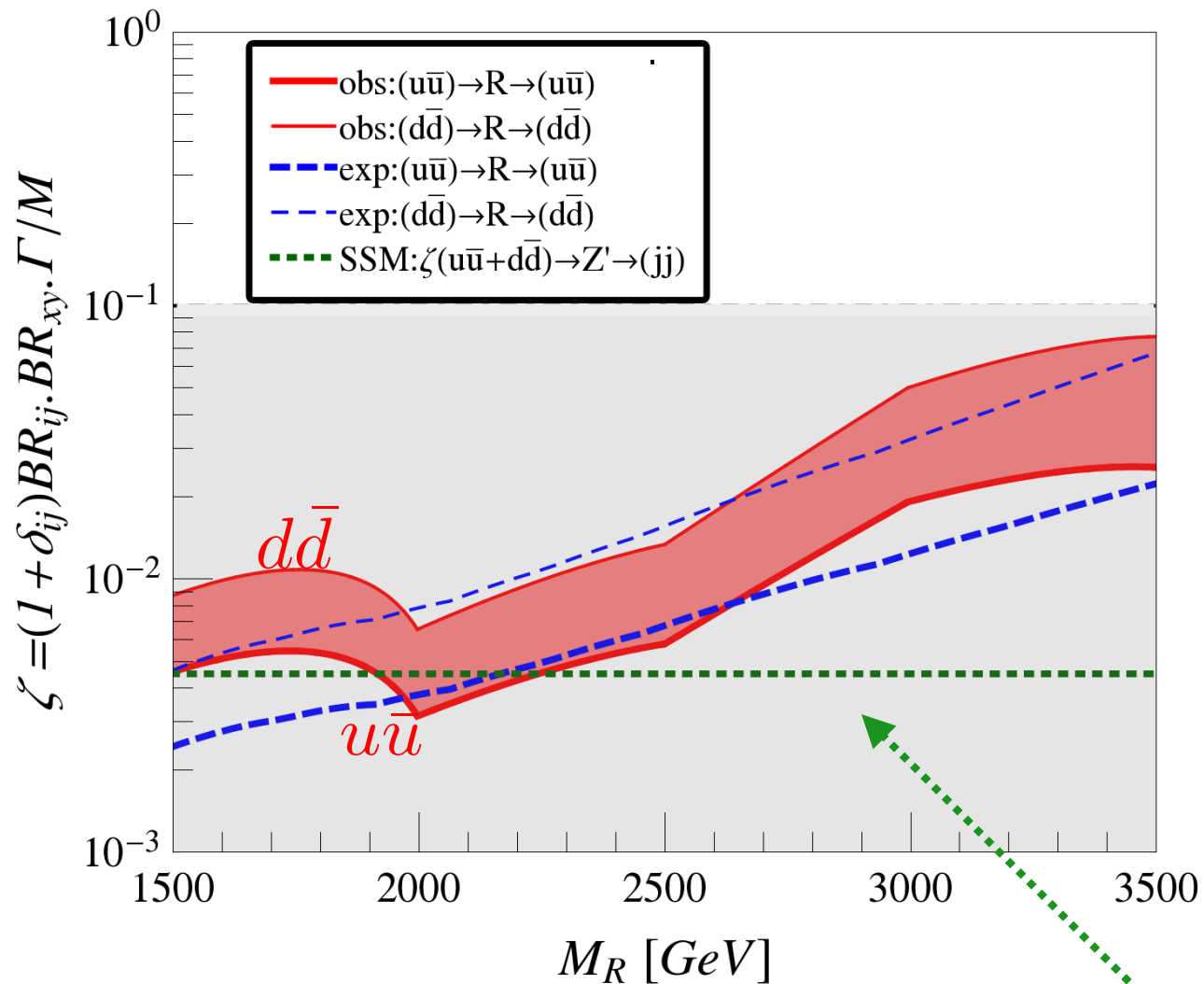


band indicates range between
Resonances (R)
coupling only to up-type quarks
vs. only to down-type quarks

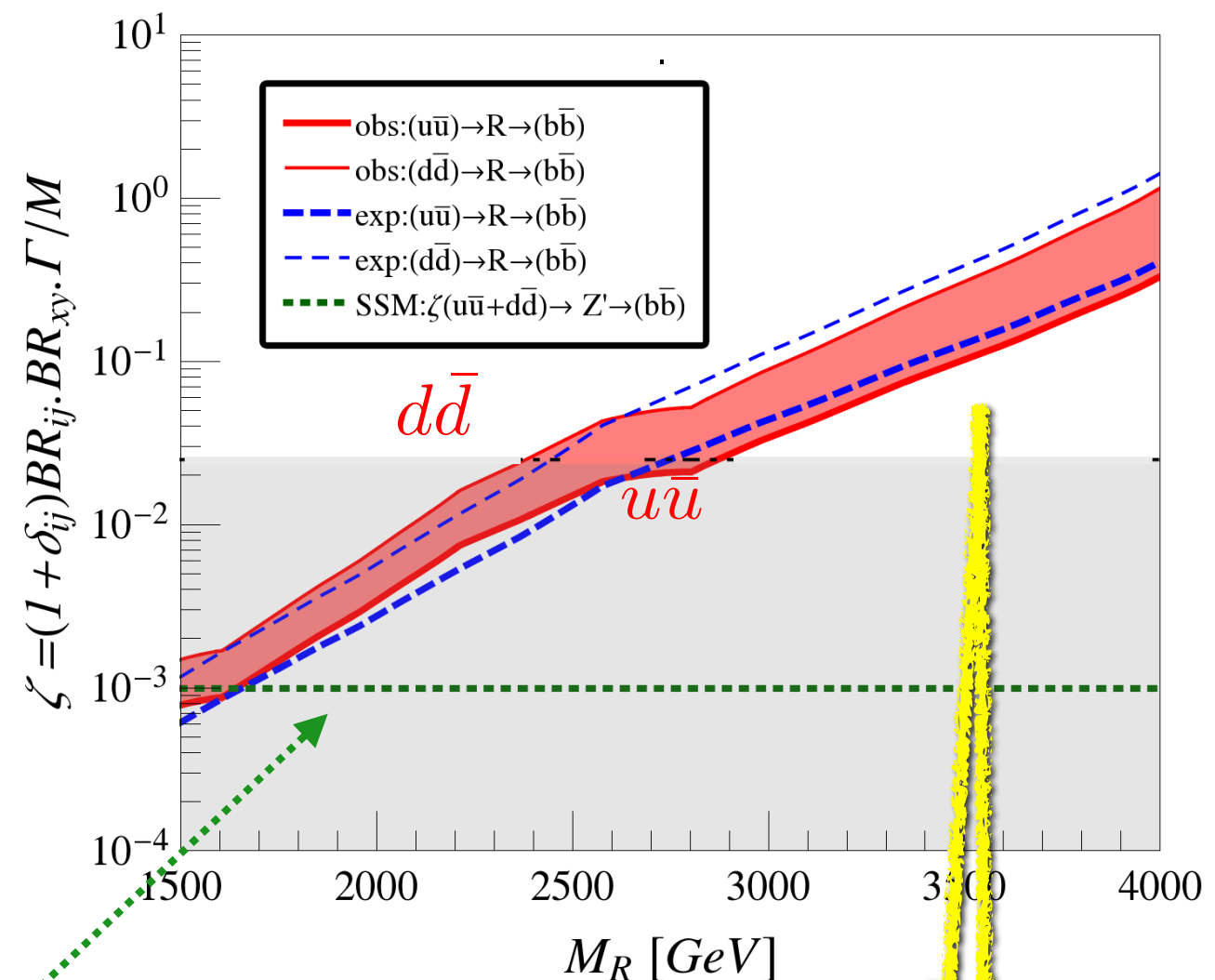
Sequential SM Z' is
excluded below ~3.5 TeV

Leptophobic Vector Resonance in Dijets

ATLAS 95% c.l. upper bounds from 3.6 fb⁻¹
at 13 TeV *Phys. Lett. B754, 302 (2016)*



ATLAS 95% c.l. upper bounds from 3.2 fb⁻¹
at 13 TeV *Phys. Lett. B759, 229 (2016)*



Sequential SM Z'

band indicates range between Resonances (R) coupling only to up-type vs. only to down-type quarks

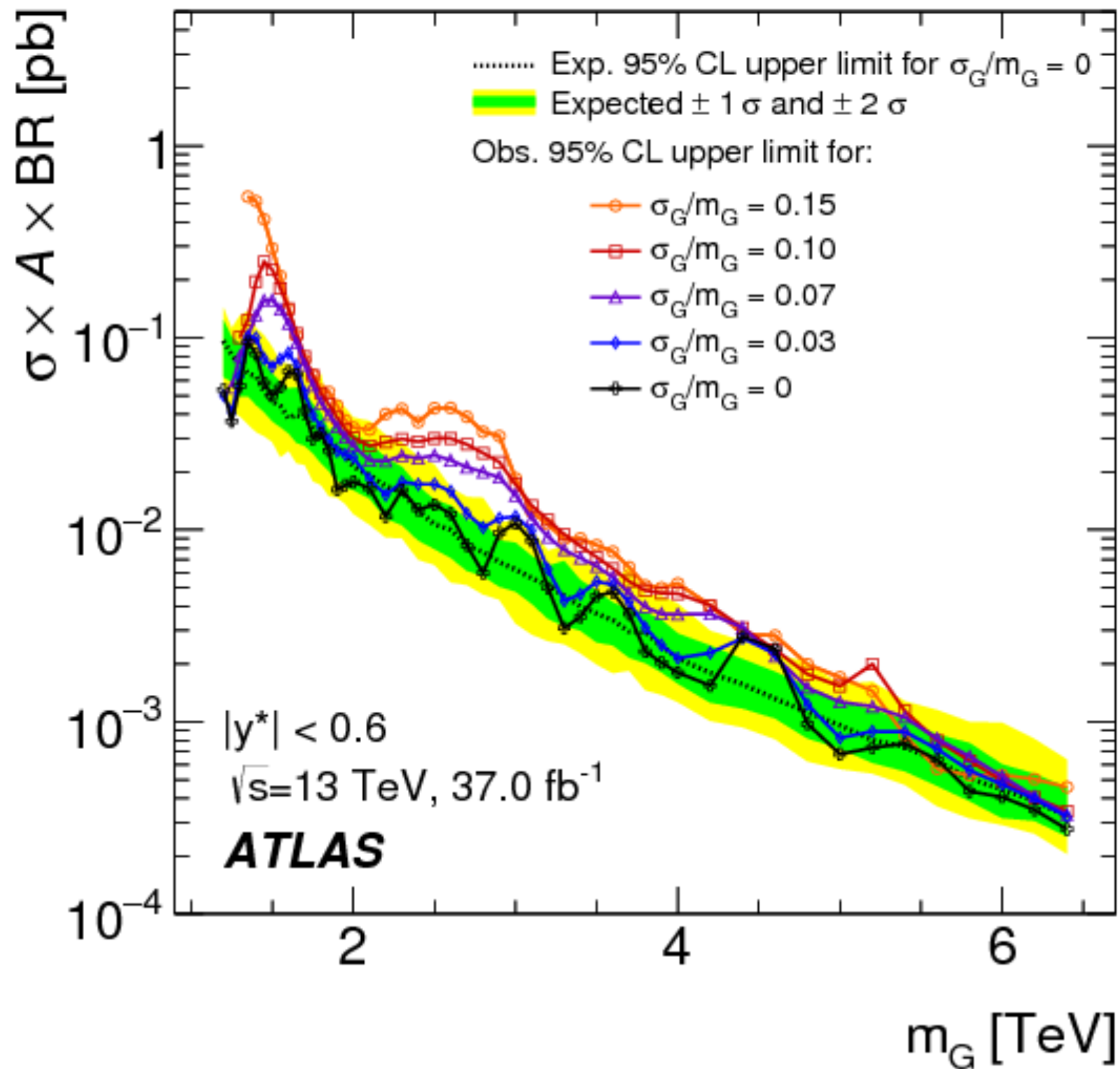
data doesn't constrain high-mass region

Simplified Limits
on s-channel resonances,
framed as bounds on

$$\zeta = BR_i BR_f \Gamma/M$$

*highlight relevant production channels
for a newly observed narrow resonance.*

Limits on finite-width resonances



Breit-Wigner Approximation

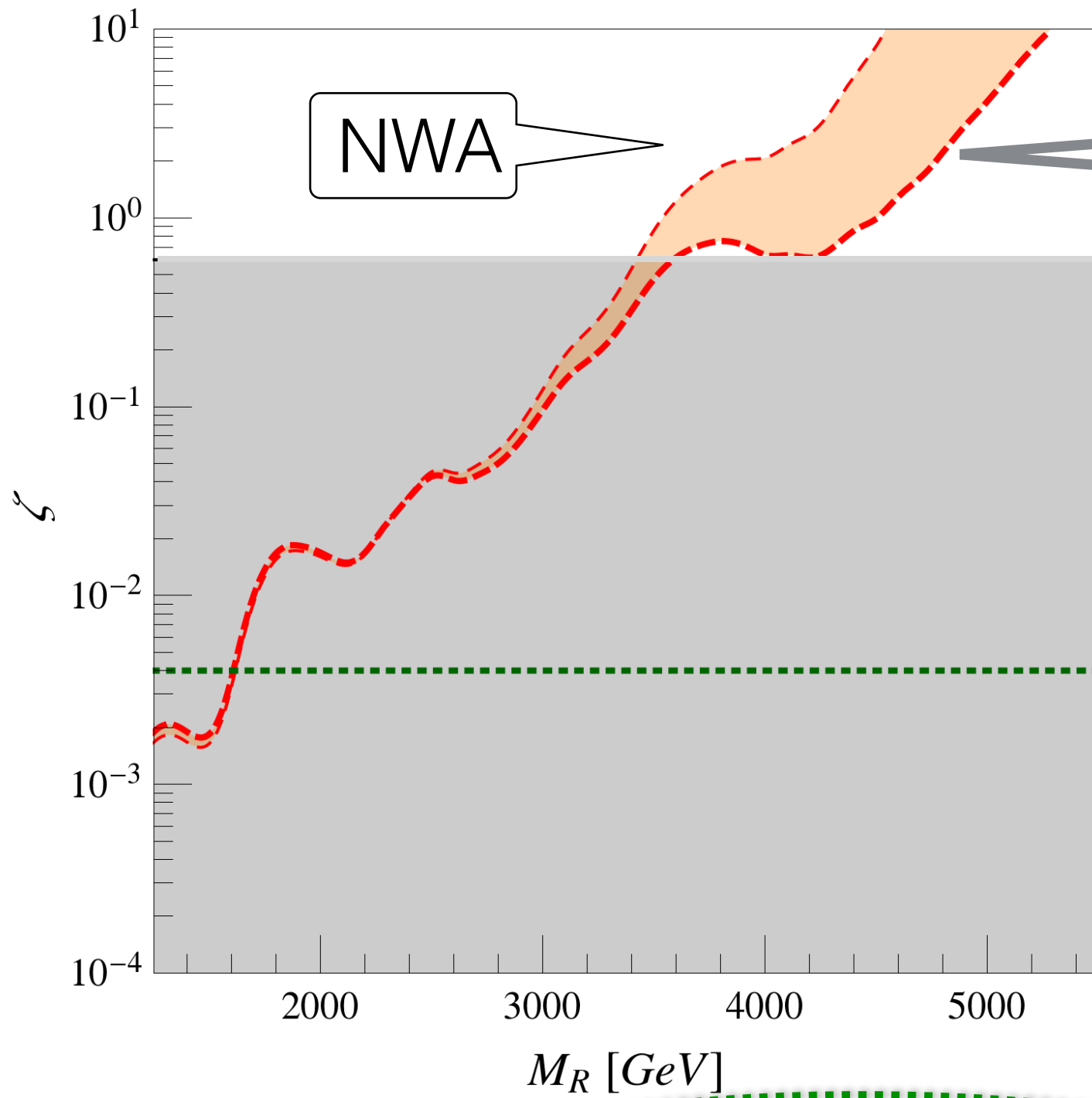
$$\sigma_R(pp \rightarrow x + y) = \int_{s_{min}}^{s_{max}} d\hat{s} \hat{\sigma}(\hat{s}) \cdot \left[\frac{dL^{ij}}{d\hat{s}} \right]$$

$$\mathcal{N} = \frac{N_{S_R}}{N_{S_i} N_{S_j}} \cdot \frac{C_R}{C_i C_j}$$

$$\hat{\sigma}(\hat{s})_{ij \rightarrow R \rightarrow xy} \equiv \frac{\Gamma_R^2}{m_R^2} \cdot \frac{\hat{s}}{m_R^4} \cdot \frac{16\pi \mathcal{N} (1 + \delta_{ij}) BR(R \rightarrow i + j) \cdot BR(R \rightarrow x + y)}{\left(\frac{\hat{s}}{m_R^2} - 1 \right)^2 + \frac{\Gamma_R^2}{m_R^2}}$$

(includes main impact of s-dependent widths)

Color-octet scalar in dijets



Breit-Wigner
 $\Gamma/M = 0.3$

$$\zeta \equiv (1 + \delta_{ij}) BR(R \rightarrow i + j) \cdot BR(R \rightarrow x + y) \cdot \frac{\Gamma_R}{m_R}$$

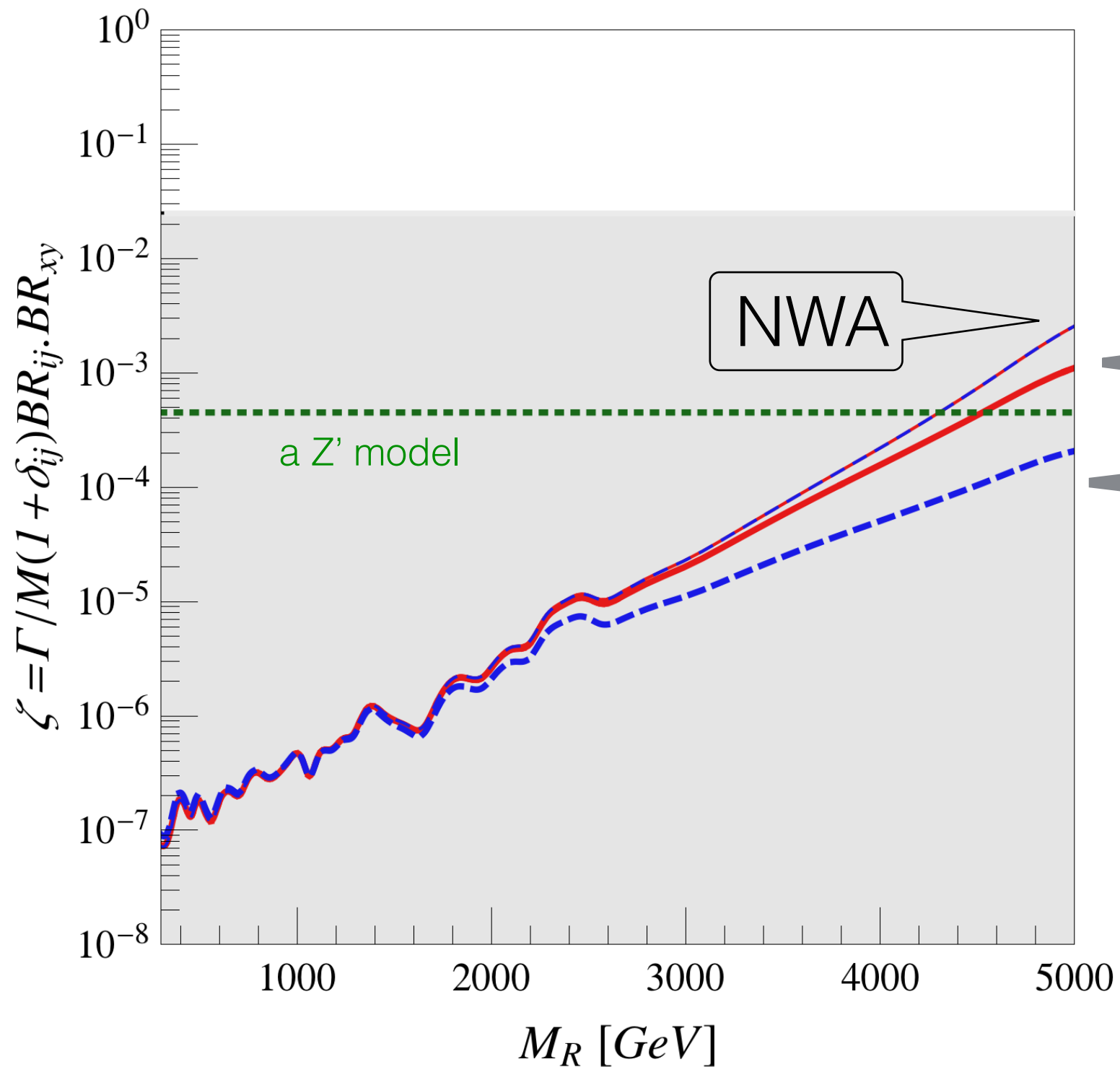
$$= \frac{\sigma_R^{XY}}{16\pi^2 \cdot \mathcal{N} \times \left[\left[\frac{1}{s} \frac{dL^{ij}}{d\tau} \right]_{\tau = \frac{m_R^2}{s}} \right]}$$

--- $gg \rightarrow R_{NWA}^{S8} \rightarrow gg$
 -.- $gg \rightarrow R_{BW}^{S8} \rightarrow gg$

-.- $gg \rightarrow S_8 \rightarrow gg: \Lambda_s = m_{S_8}, k_s = 0.1$

red curves are **CMS** 95% c.l. upper bounds from 19.7 fb⁻¹ at 8 TeV
Phys. Rev. D 91, 052009 (2015)

Vector resonance in dileptons



Breit-Wigner
 $\Gamma/M = 0.03$

Breit-Wigner
 $\Gamma/M = 0.3$

ATLAS 95% c.l. upper bounds
from 13.3 fb^{-1} at 13 TeV
ATLAS-CONF-2016-045

Simplified Limits

readily extend to finite-width resonances.

The corresponding bound from the narrow-width approximation is generally a conservative estimate of the strength of the limit.

Benefits of Simplified Limits approach

- focus on model classes \Leftrightarrow production mechanisms
- easily identify
 - exclusion limits on BSM resonances
 - whether data constrains a given channel
 - classes of models relevant for a given excess
 - [specific theories consistent with an excess]
- ζ derives directly from model parameters
- works for narrow or finite-width resonances

If collaborations report results in terms of ζ , as well as σ^*BR , it will speed and deepen our understanding of new findings.

Low-energy tail of broad peaks

